24th COBEM - 2017

24th ABCM International Congress of Mechanical Engineering
December 3-8, 2017, Curitiba, PR, Brazil

COBEM-2017-0916
NUMERICAL INVESTIGATION OF VISCOELASTIC LIQUID CURTAIN BREAKUP

Marisa S. Bazzi
Marcio S. Carvalho
Pontifical Catholic University of Rio de Janeiro - Rio de Janeiro, RJ - Brazil
mmbazzi@gmail.com
msc@puc-rio.br

Abstract. *The stability of thin liquid sheets is crucial for the success of many industrial processes, such as curtain coating applications. This stability is influenced by the type of disturbance that might emerge in the sheet and the properties of the fluid used. Previous experimental studies have shown that non-Newtonian fluids create more stable thin liquid sheets, however, the physical phenomenon responsible for this stability is not fully understood. This work addresses a numerical study of the influence of non-Newtonian properties on the stability of a thin liquid sheet. Using the Oldroyd-B model to describe a viscoelastic fluid on the influence of planar and axisymmetric perturbations, it was possible to observe that the viscoelastic properties, given by the number of Deborah and viscosity ratio of the polymer to the solvent, slow down the growth rate of perturbation leading to greater rupture time. We also investigated the influence of the perturbation type on liquid curtain stability through a linear stability analysis for a Newtonian fluid under an axisymmetric perturbation and compared to the numerical solution.The results suggest a lower stability criterion but higher growth rates for the axisymmetric perturbation compared with a planar perturbation.*

Keywords: *Thin liquid films, Oldroyd-B model, Stability analysis, Numerical simulation*

1. INTRODUCTION

Thin liquid sheets are involved in a wide range of practical applications such as atomization, paper manufacturing, and curtain coating. Regardless of the application, to achieve an efficient process it is necessary to maintain the liquid sheet stable. However, the stability of a thin liquid sheet is still a challenge for the industry, since even a small perturbation, under certain circumstances, can grow and cause the liquid sheet to break apart.

Since the pioneering study of Taylor (1959) on the dynamics of thin sheets of liquids, there have been a number of analyses concerned with the instability of a thin liquid sheet.Vrij (1966) investigated the possible mechanisms for the spontaneous rupture of thin free liquid film. Based on a simple model for a Newtonian fluid that takes into account the pressure balance and mass conservation principle, his work proposed an equation to describe the thickness fluctuation and a breakup time for ultra-thin film thickness.

Erneux and Davis (1993) applied the linear stability analysis on the linearized evolution equation for the longitudinal component of velocity and the thickness of the film and found a linear stability criterion for a Newtonian fluid based on the relation between surface tension and van der Waals force. Following this work, Ida and Miksis (1996) solved numerically the set of a partial differential equation for a two-dimensional Newtonian thin free film and were able to identify a similarity form for the film thickness and transverse velocity near to the rupture.

Nevertheless, if the fluid has a more complicated rheology properties, as most of the coating liquids, the force balance becomes more complex. For viscoelastic fluids, which contain long flexible molecules, a viscoelastic tensile will appear because of the strong planar extensional flow that occurs due to the liquid acceleration near to the rupture region. In 2010, motivated by the curtain coating process, Becerra and Carvalho (2011) presented an experimental study on curtain breakup for a high molecular weight polymer in a dilute regime. Through this study they have found that the apparent extensional viscosity of the liquids leads to a higher normal stress that stabilizes the curtain.

In 2015, in order to understand the mechanism of atomization of gel propellants, Yang *et al.* (2015) investigated the breakup characteristics of a free-surface power-law liquid sheet through a linear stability model applied to a 2-D thin liquid film. They observed that as shear rate viscosity increases the disturbance growth rate decreases. Hence, the viscous dissipation substantially affects the flow stability.

As discussed, previous works have shown that non-Newtonian properties actually play an important role in the stabilization of a thin liquid film, but little is known about the physical mechanism associated with the stabilization. Trying to elucidate the physical phenomena that cause non-Newtonian properties of liquids to stabilize a thin film, especially viscoelasticity, this work addresses a numerical analysis of two-dimensional conservation equations for a Newtonian and Oldroyd-B fluid. Benefiting from the slenderness of the fluid film, the problem is analyzed using the long wavelength theory, which is based on an asymptotic reduction of governing equations and boundary conditions to a simplified system in terms of the local thickness and velocity of the fluid film. The resulting nonlinear coupled equation system is solved for planar and axisymmetric perturbations using finite difference method.

2. MATHEMATICAL FORMULATION

The curtain liquid is bounded by a passive gas, and it is thin enough that the van der Waals forces are significant. The flow is considered two-dimensional and isothermal. As a continuum medium, the flow is governed by conservation equations which are given by the mass conservation principle and Cauchy equation of motion with an additional term related to the van der Waals component, namely

$$\frac{D\rho}{Dt} + \rho\nabla\cdot\mathbf{u} = 0 \tag{1}$$

and

$$\rho\frac{D\mathbf{u}}{Dt} = \nabla\mathbf{T} + \nabla\phi. \tag{2}$$

Boundary conditions are given by normal and tangential stress at $z = h/2$, respectively,

$$\mathbf{n}\cdot(\mathbf{n}\cdot\mathbf{T}) = \sigma\kappa \tag{3}$$

$$\mathbf{t}\cdot(\mathbf{n}\cdot\mathbf{T}) = 0. \tag{4}$$

And the kinematic condition is written as:

$$\mathbf{n}\cdot\mathbf{u} = h_t. \tag{5}$$

In equations 1 and 2, $\mathbf{u}$ is the velocity field, ρ is the fluid density, $\mathbf{T}$ is the stress tensor and ϕ is the Van der Waals potential. In 3 and 4, $\mathbf{n}$ is the normal unit vector and $\mathbf{t}$ is the tangential unit vector, σ is the surface tension which is assumed to be constant, κ is the curvature of the free surface and in Eq.5, h_t is the temporal rate of the thickness evolution.

The stress tensor $\mathbf{T}$ is composed by an isotropic part $-p\mathbf{I}$ and a non-isotropic part τ. The non-isotropic part which can be also termed *deviatoric stress tensor* has the distinctive property of being due entirely to the existence of the motion of the fluid. The stress depends on the local properties of the fluid and the instantaneous velocity field as described by Batchelor (2000). In the case of a Newtonian fluid, the deviatoric stress tensor has a linear relation with the rate of strain. For liquids of complex molecular structure, in particular for those consisting of long molecular chain that exhibit viscoelastic behavior, the deviatoric stress is more complicated once the anisotropy and the strain history become important. Due to this challenge, there is no single model available in the literature able to describe all viscoelastic fluids, instead there are several models which depend on the fluid microstructure and the type of flow.

One of the simplest yet still complex models available is the Oldroyd-b model. In this model,the deviatoric stress tensor $\boldsymbol{\tau}$ is written as superposition of solvent and polymer contributions, $\boldsymbol{\tau}= \boldsymbol{\tau_s} + \boldsymbol{\tau_p}$. The solvent constitutive equation follows Newtonian's law, $\boldsymbol{\tau_s} = \eta_s\dot{\boldsymbol{\gamma}}$. For the polymeric term, in order to introduce memory and stress anisotropy and also maintain the independence of the framework, the constitutive equation is written in a convected derivative system, given by the upper-convected Maxwell model as presented by Bird *et al.* (1977), namely

$$\boldsymbol{\tau_p} + \lambda \overset{\nabla}{\boldsymbol{\tau_p}} = \eta_p\dot{\boldsymbol{\gamma}} \tag{6}$$

where λ is the relaxation time and $\overset{\nabla}{\boldsymbol{\tau_p}}$ is the convected time derivative or contravariant that, for symmetric $\boldsymbol{\tau}$, is defined by

$$\overset{\nabla}{\boldsymbol{\tau_p}} = \frac{D}{Dt}\boldsymbol{\tau_p} - (\boldsymbol{\tau}\cdot\boldsymbol{\nabla v})^T - (\boldsymbol{\tau}\cdot\boldsymbol{\nabla v}). \tag{7}$$

Equations 1, 2 and 6 are solved using Cartesian coordinate system for planar perturbation, and cylindrical coordinate system for axisymmetric perturbation, as sketched in Figs.1 and 2. The film thickness is h and the free-surfaces are located at $y/z = \frac{h_\pm}{2}$.

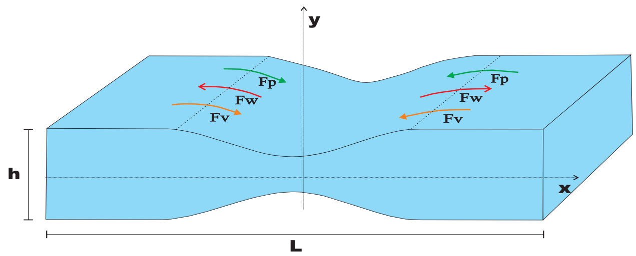

Figure 1. Planar perturbation model

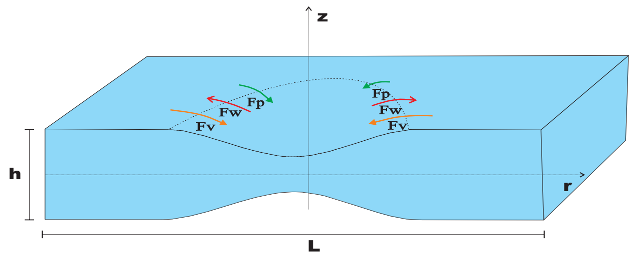

Figure 2. Axisymmetric perturbation model

2.1 Lubrication approximation

The presence of free boundaries increases the complexity of the mathematical problem. However, the slenderness of the fluid film leads to large ratio of characteristics lengths along the directions parallel and perpendicular to the flow, and the problem can be analyzed using the long wavelength theory, since variations along the film are much more gradual than those along the normal direction.

Here we describe the mathematical formulation for the axisymmetric model since the planar follows the same idea. For a two dimensional problem Eqs. 1 and 2 in cylindrical coordinates are written respectively as (Panton (2006)):

$$\frac{\partial}{\partial r}(Ur) + \frac{\partial}{\partial z}(Vr) = 0 \tag{8}$$

$$\rho\left(\frac{\partial U}{\partial t} + U\frac{\partial U}{\partial r} + V\frac{\partial U}{\partial z}\right) = -\frac{\partial P}{\partial r} - \frac{\partial \Phi}{\partial r} + \frac{1}{r}\frac{\partial}{\partial r}(r\tau_{rr}) + \frac{\partial}{\partial z}\tau_{zr} - \frac{\tau_{\theta\theta}}{r} \tag{9}$$

$$\rho\left(\frac{\partial V}{\partial t} + U\frac{\partial V}{\partial r} + V\frac{\partial V}{\partial z}\right) = -\frac{\partial P}{\partial r} - \frac{\partial \Phi}{\partial r} + \frac{1}{r}\frac{\partial}{\partial r}(r\tau_{zr}) + \frac{\partial}{\partial z}\tau_{zz}. \tag{10}$$

For an axisymmetric slender sheet, symmetric about $z = 0$, we can follow the approach used by Savva and Bush (2009) and use a Taylor expansion about $z = 0$ to write:

$$\begin{aligned}
U(r,z,t) &= u(r,t) + u_2(r,t)z^2 + ... \\
V(r,z,t) &= v_1(r,t)z + v_3(r,t)z^3 + ... \\
P(r,z,t) &= p(r,t) + p_2(r,t)z^2 + ... \\
\Phi(r,z,t) &= \phi(r,t) + \phi_2(r,t)z^2 + ... \\
\tau_{rr}(r,z,t) &= \tau_{rr}(r,t) + \tau_{rr,2}(r,t)z^2 + ... \\
\tau_{zr}(r,z,t) &= \tau_{zr}(r,t)z + \tau_{zr,2}(r,t)z^3 + ... \\
\tau_{zz}(r,z,t) &= \tau_{zz}(r,t) + \tau_{zz,2}(r,t)z^2 + ...
\end{aligned}$$

Replacing the above expansion in Eqs. 8 and 9, matching the powers of z and taking the lowest orders in z, the equations are reduced to:

$$v_1 = -\frac{\partial u}{\partial r} - \frac{u}{r} \tag{11}$$

$$\rho\left(\frac{\partial u}{\partial t} + u\frac{\partial u}{\partial r}\right) = -\frac{\partial p}{\partial r} - \frac{\partial \phi}{\partial r} + \frac{1}{r}\frac{\partial \tau_{rr}}{\partial r} + \tau_{zr} - \frac{\tau_{\theta\theta}}{\partial r}. \tag{12}$$

Normal and tangential vectors to the free surface are defined respectively as: $\mathbf{n} = [\frac{\partial h}{\partial r}\hat{e_r}, 1\hat{e_z}]$ $\mathbf{t} = [1\hat{e_r}, -\frac{\partial h}{\partial r}\hat{e_z}]$. Combining Taylor expansion with Eqs. 3 and 4 in two dimensional form, the normal and tangential boundary conditions and kinematic condition are written as:

$$\left[\left(\frac{\partial h}{\partial r}\right)^2(\tau_{rr} - p) + \frac{\partial h}{\partial r}\tau_{zr}h + \tau_{zz} - p\right]\left[1 + \left(\frac{\partial h}{\partial r}\right)^2\right]^{-1} = \sigma\kappa \tag{13}$$

$$\left[\frac{\partial h}{\partial r}\tau_{rr} + \left[1 - \left(\frac{\partial h}{\partial r}\right)^2\right]\tau_{rz}h - \frac{\partial h}{\partial r}\tau_{zz}\right]\left[1 + \left(\frac{\partial h}{\partial r}\right)^2\right]^{-1} = 0 \tag{14}$$

$$\frac{\partial h}{\partial t} + u\frac{\partial h}{\partial r} - v_1 h = 0. \tag{15}$$

In the long wavelength limit $h >> \frac{\partial h}{\partial r}$, so we can consider that $\left(\frac{\partial h}{\partial r}\right)^2 \approx 0$, Eqs. 13 and 14 become:

$$-p = \sigma\kappa - \frac{\partial h}{\partial r}\tau_{rz}h - \tau_{zz} \tag{16}$$

$$\tau_{zr}h = -\frac{\partial h}{\partial r}\tau_{rr} + \frac{\partial h}{\partial r}\tau_{zz} \tag{17}$$

and the curvature of the boundary can be approximated to:

$$\kappa = \frac{\frac{1}{2}\frac{\partial^2 h}{\partial r^2}}{(1+\frac{1}{4}(\frac{\partial h}{\partial r})^2)^{3/2}} + \frac{\frac{1}{2}\frac{\partial h}{\partial r}}{r(1+\frac{1}{4}(\frac{\partial h}{\partial r})^2)^{1/2}} \approx \frac{1}{2}\frac{\partial^2 h}{\partial r^2} + \frac{1}{2r}\frac{\partial h}{\partial r}. \tag{18}$$

From resulting Eqs.16 and 17 we find that pressure can be written as $-p = \sigma\kappa - \tau_{zz}$. And finally, we introduced nondimensional variables using the following scales:

$$r = Lr^* \quad h = Hh^* \quad u = \frac{\eta}{\rho L}u^* \quad t = \frac{\rho L^2}{\eta}t^* \quad \tau_{rr} = \frac{\eta^2}{L\rho}\tau^*_{rr} \quad \tau_{zz} = \frac{\eta^2}{L\rho}\tau^*_{zz} \quad \tau_{\theta\theta} = \frac{\eta^2}{L\rho}\tau^*_{\theta\theta} \tag{19}$$

And we can writte the non dimensional couple system of nonlinear evolution equations for the longitudinal component of velocity, the thickness of the film and the extra tension components due to the polymeric part as:

$$\frac{\partial h}{\partial t} + \frac{1}{r}\frac{\partial}{\partial r}(hru) = 0 \tag{20}$$

$$\frac{\partial u}{\partial t} + u\frac{\partial u}{\partial r} - 3S\left(\frac{\partial^3 h}{\partial r^3} + \frac{1}{r}\frac{\partial^2 h}{\partial r^2} - \frac{1}{r^2}\frac{\partial h}{\partial r}\right) - \frac{3\hat{A}}{8h^4}\frac{\partial h}{\partial r} -$$
$$\frac{4}{h}\left[\frac{\partial}{\partial r}\left(\frac{h}{r}\frac{\partial}{\partial r}(ur)\right) - \frac{u}{2r}\frac{\partial h}{\partial r}\right] + \frac{1}{r}\frac{\partial}{\partial r}(h\tau_{zz}) - \frac{1}{hr}\frac{\partial}{\partial r}(hr\tau_{rr}) + \frac{\tau_{\theta\theta}}{r} = 0 \tag{21}$$

$$\tau_{rr} + De\left(\frac{\partial \tau_{rr}}{\partial t} + u\frac{\partial \tau_{rr}}{\partial r} - 2\tau_{rr}\frac{\partial u}{\partial r}\right) = -2\eta_r\frac{\partial u}{\partial r} \tag{22}$$

$$\tau_{zz} + De\left(\frac{\partial \tau_{zz}}{\partial t} + u\frac{\partial \tau_{zz}}{\partial r} + \frac{\tau_{zz}}{r}\frac{\partial}{\partial r}(ru)\right) = -\frac{2\eta_r}{r}\frac{\partial}{\partial r}(ru) \tag{23}$$

$$\tau_{\theta\theta} + De\left(\frac{\partial \tau_{\theta\theta}}{\partial t} + u\frac{\partial \tau_{\theta\theta}}{\partial r} - 2\tau_{\theta\theta}\frac{u}{r}\right) = +2\eta_r\frac{u}{r}. \tag{24}$$

Where $S = \frac{\sigma H\rho}{6\eta^2}$ is a non dimensional parameter associated with the ratio of inertia, viscous and surface tension forces. $\hat{A} = \frac{A\rho l^2}{6\pi H^3\eta^2}$ is a non dimensional parameter that encompasses the effects of the van der Waals forces through the Hamaker constant, $De = \frac{\lambda\eta}{L^2\rho}$ is the Deborah number that measures the ratio of the relaxation time of the liquid to a characteristic time of the flow, and $\eta_r = \frac{\eta_p}{\eta}$ that is the ratio of the polymeric and solvent viscosity .

2.2 Linear stability criterion

Erneux and Davis (1993) have shown that an uniform thickness sheet is linearly stable when the ratio between the non-dimensional surface tension and non-dimensional van der Waals force are larger than two over the square of wave number of the perturbation, i.e. $S/A = 2/a_c^2$, where $a_c = \pi/L$

Following the same procedure, we can find a stability criterion for the axisymmetric model. Considering the steady-state solution $(\bar{u}, \bar{h}) = (0, 1/2)$ and by introducing the deviations $h' = h - 1/2$ and $u' = u$ we obtain the following linearized system for the Newtonian model:

$$\frac{\partial h'}{\partial t} + h'\frac{\partial u'}{\partial r} = 0 \tag{25}$$

$$\frac{\partial u'}{\partial t} - 3S\left(\frac{\partial^3 h'}{\partial r^3} + \frac{1}{r}\frac{\partial^2 h'}{\partial r^2} - \frac{1}{r^2}\frac{\partial h'}{\partial r}\right) - \frac{3A}{8h^4}\frac{\partial h'}{\partial r} - 4\frac{\partial^2 h'}{\partial r^2} - \frac{4}{r}\frac{\partial u'}{\partial r} = 0. \tag{26}$$

Equations 25 and 26 accept solution of the form:

$$(h', u') = (h_0, u_0)e^{\omega t + i\alpha x} \tag{27}$$

where ω is the growth rate and α is the wave number. We substitute Eq. 27 into Eqs. 25 and 26 and taking the real part, we can find the following equation for ω:

$$\omega^2 + 4\omega\alpha^2 + \frac{3}{2}\alpha^2\left(S\alpha^2 + \frac{4S}{L^2} - 2A\right) = 0. \tag{28}$$

The equation admits a zero ω is the last coefficient is equal to zero, which leads to the "cutoff" wave number for the axisymmetric model:

$$\alpha_c = \sqrt{\frac{2A}{S} - \frac{4}{L^2}}. \tag{29}$$

For a wave number equal to $\alpha_c = \pi/L$, then we have that the stability criterion for an axisymmetric model is given by:

$$\frac{A}{S} = \frac{2L^2}{\pi^2 + 4}. \tag{30}$$

The additional term that appears in the denominator is due to the extra curvature of the axisymmetric model. Thus, this result suggests that, due to this extra curvature, a smaller surface tension is needed to stabilize an axisymmetric perturbation. The ratio $(S/A|_a)/(S/A|_p) = \pi^2/(\pi^2 + 4) = 0.71$ proposes that this value is 71% smaller.

2.3 Numerical approximation

A numerical approximation of the solutions of the transport equations was obtained by using the Finite Difference Method (FDM). The method consists of approximating derivatives of the differential equation via truncated Taylor series. A staggered mesh over the interval $0 < r < 1$ was used to avoid spurious oscillations in the curvature in the long-time limit as suggested by Savva and Bush (2009), the values of h_i are prescribed at r_i and the values of u_i are prescribed at $r_{i+1/2}$. To obtain a better spatial accuracy in the region near the rupture, a concentrated mesh was implemented. The result is a sparse set of coupled, nonlinear algebraic system equations, which was solved using Newton's method with a numerical Jacobian matrix with a second-order central difference scheme. The time integration was performed with the Crank-Nicholson method.

The numerical solution was validated using the Newtonian planar model and matching results with Ida and Miksis (1996). Figure 3 shows the mesh convergence for a number of elements larger than 200.

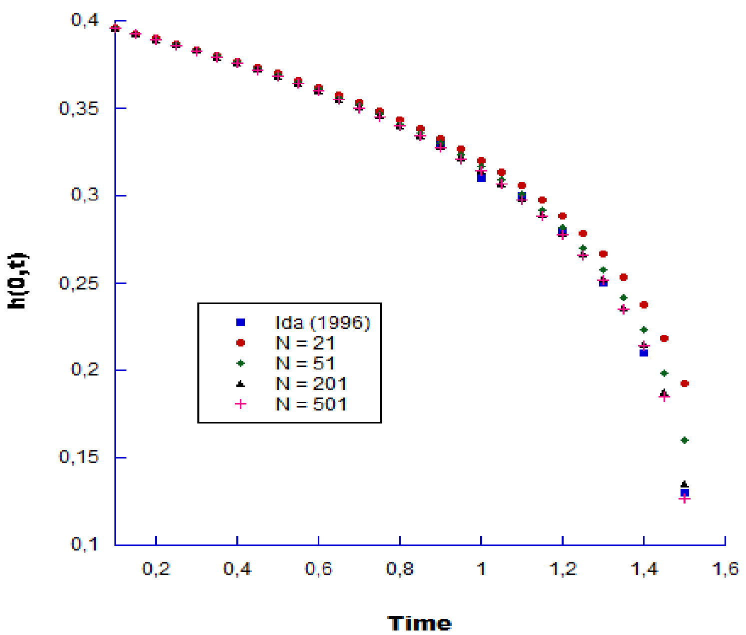

Figure 3. Mesh test for planar perturbation model in a Newtonian fluid.

Figures 4 and 5 compare the evolution of the time thickness obtained from the numerical solution with the profile suggested by Ida and Miksis (1996).

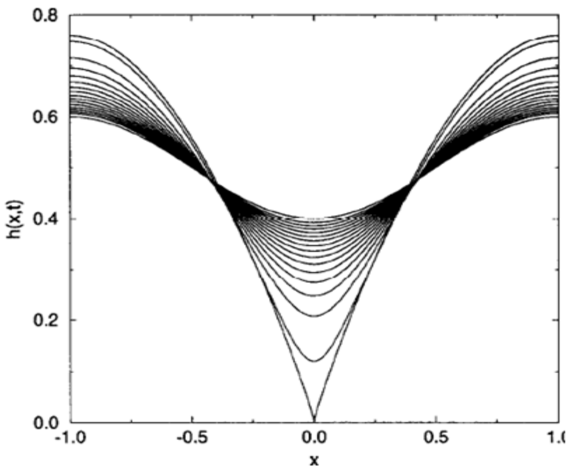

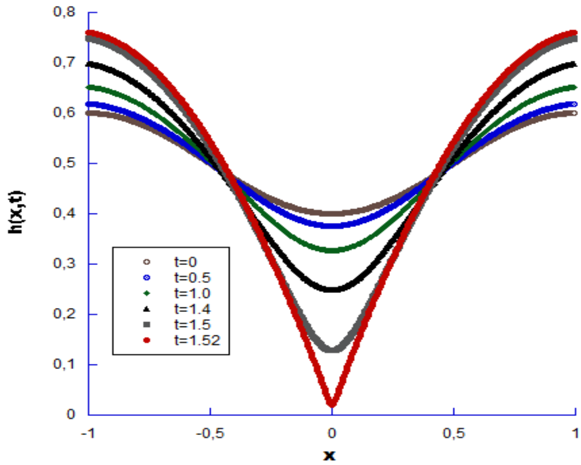

Figure 4. Thickness evolution profile Ida and Miksis (1996). Figure 5. Numerical solution for thickness evolution profile.

The initial conditions are fixed for all models and equal to $(h(x,0), u(x,0)) = (1/2 - \epsilon cos(\alpha_c x), 0)$, where ϵ is a small perturbation in the steady-state solution and chosen to be 2% of the mean thickness.

3. RESULTS

First, we numerically investigate the stability criteria for planar and axisymmetric model by examining the perturbation growth for different values of the parameter $S/A = 3\pi\sigma H^4/L^2 A$. This parameter represents a relation between surface tension and van der Waals forces. Typical values of the van der Waals force and surface tension for water-like liquids in thin sheets lead this ratio to values in a range of $S/A = 1/100\pi^2$ to $S/A = 10/\pi^2$ depending on the thickness and the length of the liquid sheet. Based on that, we set a range of values from $S/A = 1/10\pi^2$ to $S/A = 3/\pi^2$ for our study.

Figure 6 shows that for values of $S/A < 1.5/\pi^2$ for the axisymmetric model and for values of $S/A < 2/\pi^2$ for the planar model , the growth rate of the perturbation is positive and a small perturbation grows leading to rupture of the curtain liquid in a finite time. This behavior matches the instability criteria described in the previous section which proposes that, for a Newtonian fluid, the extra curvature in the axisymmetric model helps stabilize the curtain liquid.

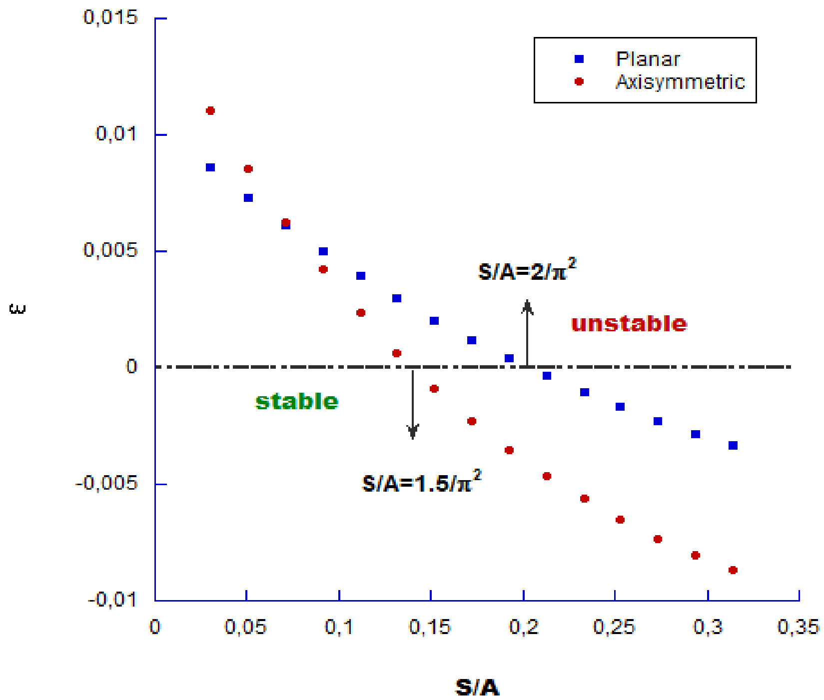

Figure 6. Stability criteria for Newtonian fluid under planar and axisymmetric perturbations.

Figure 6 also shows that the growth rate of the perturbation for planar and axisymmetric models are slightly different. For values of S/A far from the stability criterion, the axisymmetric model seems to have a higher growth rate which leads to a lower rupture time. In order to investigate this in more detail, we analyze the rupture time for a parameter $S/A = 1/10\pi^2$, in fact, as shown in Fig. 7 the axisymmetric perturbation leads to a faster rupture of the curtain.

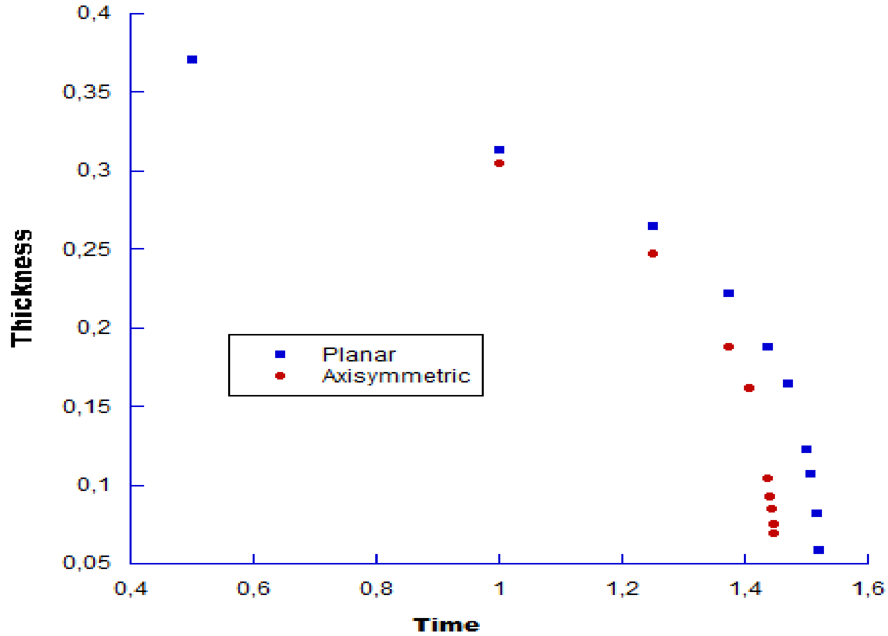

Figure 7. Rupture time analyses for $S/A = 1/10\pi^2$.

To investigate the effects of the non-Newtonian properties, we first studied the effect of the ratio between the polymeric and solvent viscosity on the stability criterion. Figures 8 and 9 show that, regardless of perturbation model, the viscoelasticity does not affect the stability criteria, but instead affects the perturbation growth rate. Increasing the viscosity ratio, raises the viscoelastic stress and hinders the growth of the perturbation, inducing a delay in rupture time. As observed by Becerra and Carvalho (2011) in the curtain coating application, such a delay might be sufficient to avoid the disintegration process of the curtain liquid, since once the rupture time reaches a value larger than the deposition time, the defect will not have enough time to propagate in liquid curtain.

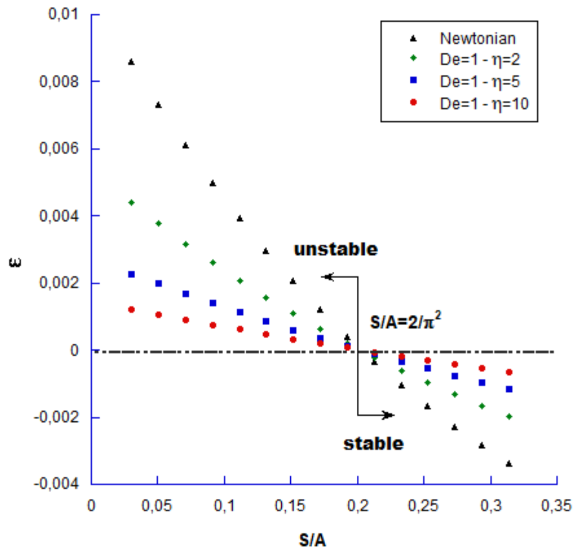

Figure 8. Stability criterion for planar model.

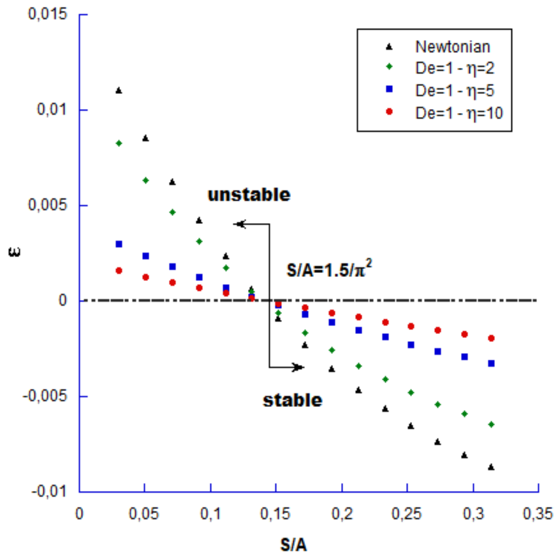

Figure 9. Stability criterion for axisymmetric model.

To examine the dependence of the rupture time on the non-Newtonian properties, we set the parameter $S/A = 1/\pi^2$ thus eliminating the influence of the van der Waals the surface tension foces. In Fig. 10, the rupture time is given as a function of the viscosity ratio and for different Deborah numbers. It is possible to observe that the rupture time is highly dependent of the Deborah number.

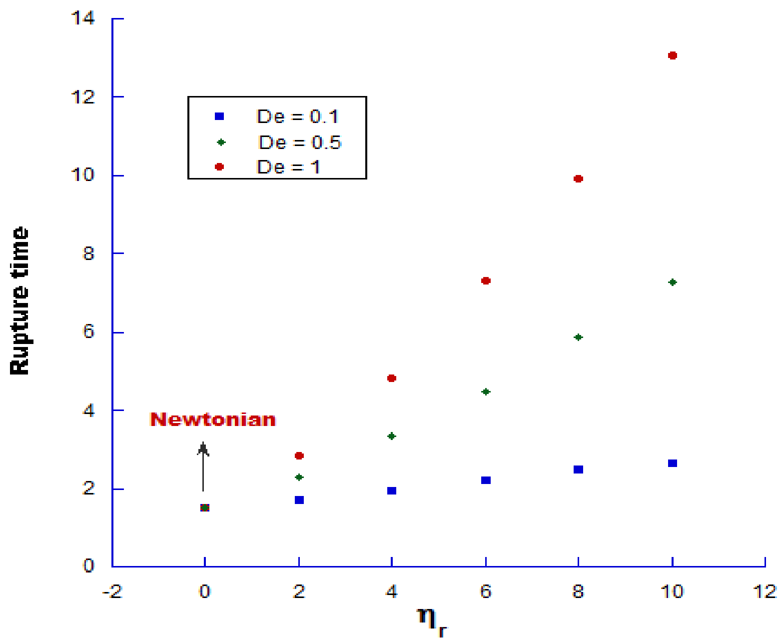

Figure 10. Viscoelastic effects in the rupture time for planar model.

4. FINAL REMARKS

A stability criterion for an axisymmetric perturbation model was proposed based on Erneux and Davis (1993). The result suggests that an axisymmetric perturbation is more stable than a planar disturbance, due to the extra curvature that helps stabilize the curtain.

The differential equation system for the thickness evolution and velocity field was solved by using finite differences method. The numerical solution showed that for low surface tension, that means S/A far from the stability criterion, the axisymmetric perturbation grows faster than the planar perturbation, leading to a lower rupture time as shown in Fig. 7.

The non-Newtonian effects were studies through the Oldroyd-B model for a fixed parameter S/A. The results suggest that viscoelasticity does not affect the stability criterion but changes the growth rate of the perturbation delaying the rupture time.

Finally, the results show that viscoelastic forces slows down the growth of perturbations, which may explain the stabilization of curtain coating process observed experimentally.

5. REFERENCES

Batchelor, G.K., 2000. *An introduction to fluid dynamics*. Cambridge university press.

Becerra, M. and Carvalho, M.S., 2011. "Stability of viscoelastic liquid curtain". *Chemical Engineering and Processing: Process Intensification*, Vol. 50, No. 5, pp. 445–449.

Bird, R.B., Armstrong, R.C., Hassager, O. and Curtiss, C.F., 1977. *Dynamics of polymeric liquids*, Vol. 1. Wiley New York.

Erneux, T. and Davis, S.H., 1993. "Nonlinear rupture of free films". *Physics of Fluids A: Fluid Dynamics*, , No. 5, pp. 1117–1122.

Ida, M. and Miksis, M., 1996. "Thin film rupture". *Applied Mathematics Letters*, Vol. 9, No. 3, pp. 35–40.

Panton, R.L., 2006. *Incompressible flow*. John Wiley & Sons.

Savva, N. and Bush, J.W., 2009. "Viscous sheet retraction". *Journal of Fluid Mechanics*, Vol. 626, pp. 211–240.

Taylor, G., 1959. "The dynamics of thin sheets of fluid. iii. disintegration of fluid sheets". In *Proceedings of the Royal Society of London A: Mathematical, Physical and Engineering Sciences*. The Royal Society, Vol. 253, pp. 313–321.

Vrij, A., 1966. "Possible mechanism for the spontaneous rupture of thin, free liquid films". *Discussions of the Faraday Society*, Vol. 42, pp. 23–33.

Yang, L.j., Du, M.l., Fu, Q.f., Tong, M.x. and Wang, C., 2015. "Temporal instability of a power-law planar liquid sheet". *Journal of Propulsion and Power*.

6. RESPONSIBILITY NOTICE

The following text, properly adapted to the number of authors, must be included in the last section of the paper:
The authors are the only responsible for the printed material included in this paper.